

Energy –Band Structure and Optical Properties of SnS Compound

Eldar Mehrali Qojayev, Jahangir Islam Huseynov

Abstract— In this paper, based on first-principles calculations within the pseudopotential theory calculated the band states of crystals SnS with rhombic lattice structure. According to the calculated band structure of the compound SnS valence band can be divided into three subgroups. Analysis of wave functions of valence states shows that the lowermost group separated from the main group of valence band by a wide energy gap about 6eV, arises from *s* – states of anion. The next group, consisting of four bands and located near-7eV is due to *s*-states of Sn. The uppermost group of twelve bands located in the range between 0 and – 5eV appears *p*-states of cation and anion. Analysis of origin valence states is suitable with photoelectron emission data. The width of forbidden zone computed using energy-band structure is suitable to its experimentally determined value. Spectral dependence of refraction index, reflection coefficient, of the real and imaginary parts of optical electric conduction, of the characteristic function of electron energy losses and the effective state density of compound for $\epsilon_{||}$ and ϵ_{\perp} polarizations have been done.

Index Terms— Energy-band structure, optical properties, valence states.

I. INTRODUCTION

The present paper contains the results of computing energy spectrum and optical functions of SnS compound. The computations were made using pseudopotential method which is one of the principal for computing energy spectrum of charge carriers of semiconductors. This method is extensively described in papers [1-6].

II. THE EXPERIMENTAL METHOD

The pseudopotential theory is based on three fundamental physical approximations.

1. The first approximation is the approximation of self-matched field. Interaction between electrons in this approximation is characterized by a particular average potential which itself depends on the states of electrons, the mentioned electron states in turn are determined by average potential.

2. In the second approximation all electron states are divided into inner shells (“the core”) and of conduction band wave functions of the inner shells are supposed to be strongly localized.

3. The third fundamental approximation is the use of perturbation theory for electrons in conduction band.

Manuscript received January 23, 2015.

Eldar M. Qojayev, Department of Physics, Azerbaijan Technical University, Baku, Azerbaijan 0503666633

Jahangir I. Huseynov, Department of Electrical and Optics, Azerbaijan State Pedagogical University, Baku, Azerbaijan 0506645227

Non-local ionic pseudopotentials in configuration space were constructed according to a scheme proposed in papers [4, 6].

Paper [7] demonstrates symmetry elements of $D_{2h}^{16}(P_{cm})$ spatial group, Brillouin zone, tables of non-reducible representations of groups of wave vectors of symmetrical points and lines of Brillouin zone and also describes rules of selecting dipole transitions for some symmetrical points and lines.

We have performed the computation of SnS compound energy-band structure by pseudopotential method. Non – local ionic pseudopotentials in configuration space were constructed according to a scheme proposed in paper [5]. When computing energy- band structure of this compound the screening of ionic charge as well as exchange – correlational effects were considered within dielectrical formalism in conformity with Hubbard –Sham’s model with some selective distribution of charge around each ion. About 2500 plane waves were used in expanding wave function. In doing so maximum kinetic energy of considered energy of plane waves was 20 Ry.

The parameters of optimized lattice:

Lattice parameters, (Å)	SnS	
	Theor.	Exper
<i>a</i>	4.246	4.334
<i>b</i>	10.943	11.200
<i>c</i>	3.922	3.987
x (cation)	0.1155	0.1198
y (cation)	0.1175	0.1194
x (anion)	0.4745	0.4793
y (anion)	0.8535	0.8508

As seen from Fig.1, valence band of SnS consists of three groups of bands. The characteristic pair wise arrangement of valence bands is consequence of crystal lamination. Analysis of wave functions of valence states shows that the lowermost group separated from the main group of valence band by a wide energy gap about 6eV, arises from *s* – states of anion. The next group, consisting of four bands and located near – 7eV is due to *s*-states of Sn. The uppermost group of twelve bands located in the range between 0 and – 5eV appears because of *p*-states of cation and anion. Analysis of origin of valence states agrees well with photoelectron emission data. The width of forbidden zone computed using energy-band structure is in good agreement with its experimentally determined value.

It is known that optical properties of SnS are not sufficiently investigated experimentally. For this reason theoretical investigation of several optical properties of the

said compound is needed. With this object in view we real parts have conducted computations of imaginary and real parts of complex dielectric penetrability in the course of polarizations of parallel and perpendicular optical axis and have computed other optical functions as well.

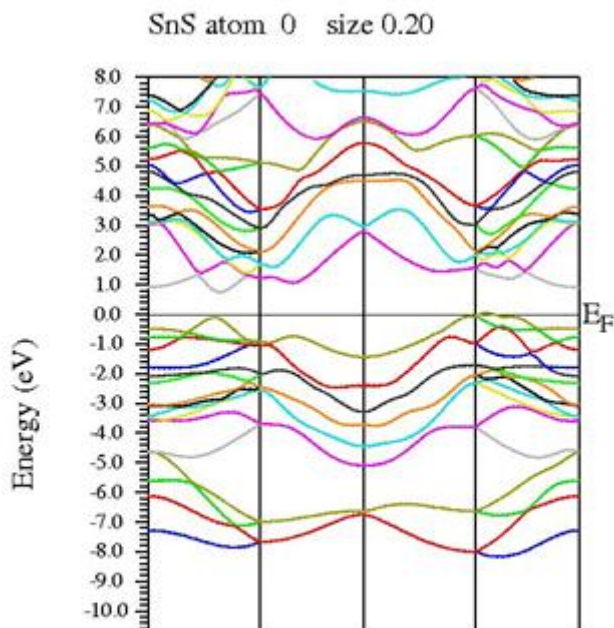


Fig.1. Energy- band structure of SnS compound

III. RESULTS AND DISCUSSIONS

When determining frequency dependence of the imaginary part of complex dielectric penetrability we have employed relation [8]:

$$\varepsilon_i(\omega) = \frac{4\pi^2 e^2}{m_e^2 \omega^2} \sum_{vc} \int_{z_B} \frac{2d^3k}{(2\pi)^3} |\mathbf{e} \cdot \mathbf{M}_{cv}(\mathbf{k})|^2 \delta(E_c(\mathbf{k}) - E_v(\mathbf{k}) - \hbar\omega), \quad (1)$$

here $\mathbf{e} \cdot \mathbf{M}_{cv}(\mathbf{k}) = \mathbf{e} \cdot \int \psi_{ck}^*(\mathbf{r})(-i\hbar\nabla)\psi_{vk}(\mathbf{r})d^3r$, where

an integral in the right part denotes matrix element of pulse operator $\mathbf{p} = -i\hbar\nabla$; indices v and c numerate states of valence band and conduction one respectively; \mathbf{k} - wave vector; \mathbf{e} – unit vector of polarization. Integration is made with respect to the volume of crystal elementary cell.

In (1) we have replaced integration with respect to BZ by summation in elementary cell of inverse lattice. In this process the elementary cell was divided into 8 part of equal volume and \mathbf{k} points were selected in these parts randomly. 1280 points were taken in all as a result of which a smooth histogram was obtained. Then this histogram was normalized by the following formula

$$\int_0^\infty \omega \varepsilon_i(\omega) d\omega = \frac{\pi}{2} \omega_p^2 = \frac{\pi}{2} \cdot \frac{4\pi n_e e^2}{m_e},$$

where ω_p - plasma frequency for electrons; n_e - average density of electrons in crystal. The computation shows that $\hbar\omega_p$ equals to 14,25 eV.

The histogram was plotted with a step of $\approx 0,2\text{eV}$. All transitions $v \rightarrow c$ with energy up to 15eV had been considered. Starting from small structure in the histogram about 15eV the $\varepsilon_i(\omega)$ dependence was extrapolated by the known formula:

$$\varepsilon_i(\omega) \Big|_{\omega \rightarrow \infty} \sim \frac{1}{\omega^3}.$$

The real part of dielectric penetrability is computed from integral dispersive Kramers-Kronig relation

$$\varepsilon_r(\omega) = 1 + \frac{2}{\pi} P \int_0^\infty \omega' \varepsilon_2(\omega') \cdot \frac{d\omega'}{\omega'^2 - \omega^2}$$

symbol P here stands for integral in a sense of the main value.

The effective number of valence electrons per atom participating in transitions with the energy of $E \leq \hbar\omega$, is determined as:

$$n_{eff} = \frac{m_e}{2\pi^2 e^2} \cdot \frac{1}{n_a} \int_0^\omega \varepsilon_i(\omega') \omega' d\omega',$$

$$n_a = \frac{N_{cell}}{V_{cell}},$$

where n_a -density of atoms in crystal; e – elementary charge; m_e - electron mass.

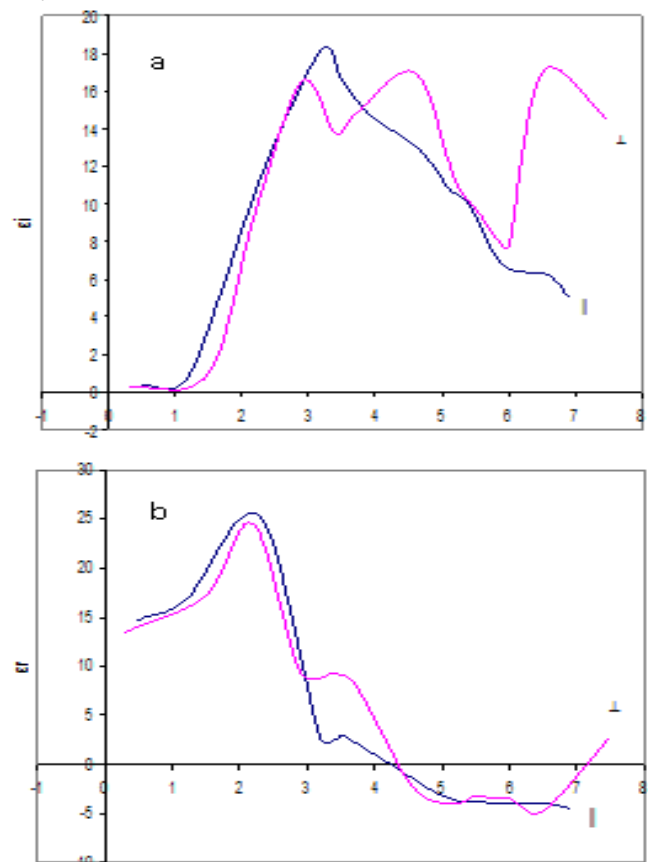


Fig.2. Spectral dependence of the imaginary (ε_i) and real (ε_r) parts of dielectrical penetrability of SnS compound for $\mathbf{e}||\mathbf{c}$ (a) and $\mathbf{e}\perp\mathbf{c}$ (b) polarizations

The results of computing the above mentioned optical constants in the 0-8 eV energy range are displayed in Figs. 2-5. As follows from Fig.2a, a maximum of the main peak in $\epsilon_r(\omega)$ spectrum at $e\parallel c$ polarization is observed when the energy is 2,20 eV, when the energy is 3,37 eV a weak maximum is noted. $\epsilon_r(E)$ goes down to the energy of 6,46 eV after which increase takes place.

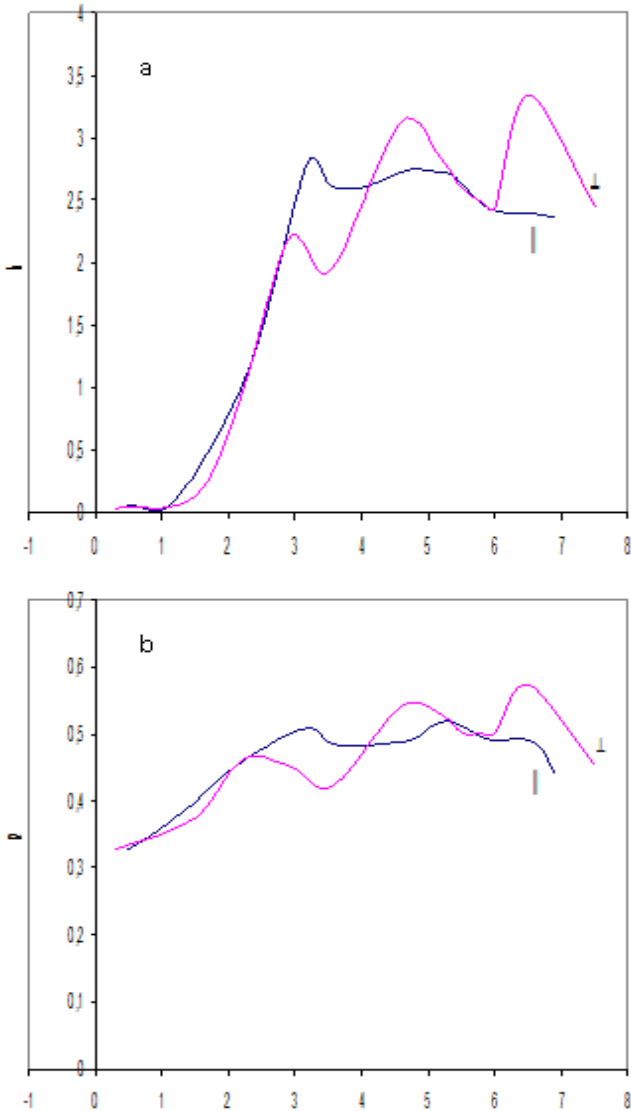


Fig.3. Energy dependence of refractive index (a) and reflection coefficient (b) of SnS compound at $e\parallel c$ and $e\perp c$ polarizations

At 4,25 eV $\epsilon_r(E)$ inversion occurs. At $e\perp c$ polarization $\epsilon_r(E)$ increases to the energy of 2,23 eV, reaching its maximum value (24,4) drops to 3,13 eV, a small growth and decrease in $\epsilon_r(E)$ are observed. Fig. 2b demonstrates dependencies of the imaginary part of dielectric penetrability $\epsilon_i(E)$ on energy at $e\parallel c$ and $e\perp c$ polarizations.

As seen from Fig.2b at $e\perp c$ polarization $\epsilon_i(E)$ at first rises to 13 when the energy is 3,4 eV, attaining a maximum and falls to 7,97 at 6,14 eV. Further, at the energy of 6,23 eV two maxima in $\epsilon_i(E)$ dependencies at $e\parallel c$ polarization happen at 3,1 and 4,6 eV and a minimum is observed at 3,54eV with a decrease in $\epsilon_i(E)$ down to 6,46.

As follows from Fig.2b, at $e\parallel c$ polarization two clearly marked maxima are seen on $\epsilon_i(E)$ curve at 3,1 and 4,66

eV and a minimum occurs at 3,54 eV. After 4.66 eV a decrease in ϵ_i takes place, ϵ_i reaches its maximum value of 13,6 when the energy is 3,4 eV. At $e\perp c$ polarization two maxima are evident on $\epsilon_i(E)$ curve at 3,4 and 6,8 eV and deep minimum at the energy of 6,14 eV is witnessed. On the whole, at both polarizations ϵ_i changes according to energy are identical.

The imaginary part of refraction index is determined by the following formula:

$$k = \sqrt{\frac{1}{2}(-\epsilon_r + \sqrt{\epsilon_r^2 + \epsilon_i^2})}$$

while reflection index at normal falling of light is determined by the formula below:

$$R = \frac{(n-1)^2 + k^2}{(n+1)^2 + k^2}$$

Fig.3 gives the results of computing refraction (k) and reflection @ indices at $e\parallel c$ and $e\perp c$ polarizations. As follows from Fig.3a, at $e\parallel c$ polarization k rises from zero to 2,8 and at the energy of 3,32 eV a slightly marked maximum and a weak decrease are observed.

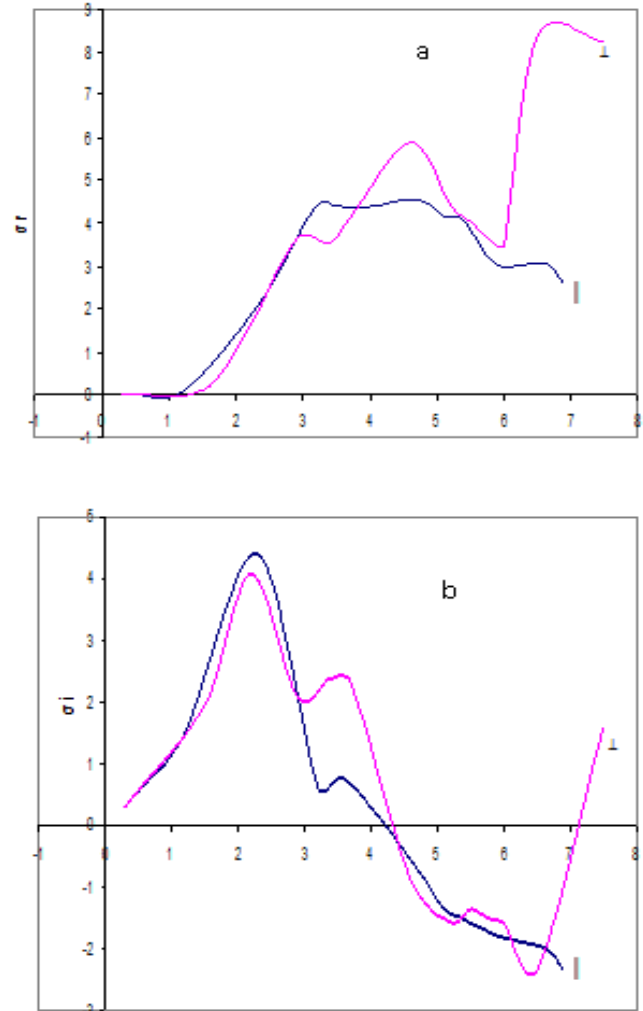


Fig.4. Spectral dependencies of the real $\alpha_r(E)$ (a) and imaginary parts $\alpha_i(E)$ (b) of optical electric conduction of SnS compound for $e\parallel c$ and $e\perp c$ polarizations

At $e_{\perp c}$ polarization two maxima are present on $k(E)$ curve at the energies of 4,79 and 6,55 eV and two minima at the energies of 3,51 and 5,97 eV, at $e_{\perp c}$ polarization an increase in k occurs from zero to 3,5 with differentials. Reflection index at $e_{\parallel c}$ polarization has two weakly marked maxima at 3,25 and 5,1 eV (Fig3b)

On the whole, R change with energy is little-from 0,35 to 0,5. At $e_{\perp c}$ polarization three maxima are witnessed on $R(E)$ curve at 2,17; 4,79 and 6,52 eV and two minima at 3,46 and 5,9eV. And in this case R change with the growth of energy takes place in the 3,5-5,5 interval.

The real and imaginary parts of optical electric conduction of SnS are found with the help of the following formulae:

$$\sigma_r = \frac{\omega \varepsilon_i}{4\pi}, \quad \sigma_i = -\frac{\omega \varepsilon_r}{4\pi}.$$

The results of computing the real and imaginary parts of optical electric conduction are given in Fig.4. As seen from Fig.4b, two weakly marked maxima are present on $\sigma_r(E)$ curve at $e_{\perp c}$ polarization when the energies are 3,28 and 6,69 eV and minimum at 5,9eV σ_r goes up in the 0-3,28 eV energy range, it remains practically constant in the 3,28-5,9 eV range, its drastic rise from 3,5 to 8,5 is observed in a narrow range from 5,9 to 6,7 eV, further a weak decrease occurs.

At $e_{\parallel c}$ polarization a structure is found on $\sigma_r(E)$ curve at 3,02 eV, a sharply marked maximum is observed at 4,59 eV and a weak maximum is present 6,57 eV. The $\sigma_r(E)$ changes at $e_{\parallel c}$ polarization in the 0-8 eV energy interval take place from zero to 6. Fig.4a shows $\sigma_i(E)$ dependencies at $e_{\parallel c}$ and $e_{\perp c}$ polarizations. As follows from Fig.4a, at $e_{\perp c}$ polarization two sharply pronounced maxima are observed on the $\sigma_i(E)$ curve at 2,23 and 3,5 eV and two minima at 3,01 and 6,41 eV. On the whole, structures and electric conduction intervals are present on the $\sigma_i(E)$ curve. A change in σ_i in the 0-8eV interval ranges from -2,5 to 4,5. At $e_{\parallel c}$ polarization two maxima are registered on the $\sigma_i(E)$ curve at 2,23 and 3,56 eV, a minimum is revealed at the energy of 3,3 eV. A change in σ_i at $e_{\parallel c}$ polarization in the energy interval under investigation ranges between -2 and 4.

$$\sigma_r = \frac{\omega \varepsilon_i}{4\pi}, \quad \sigma_i = -\frac{\omega \varepsilon_r}{4\pi}.$$

The characteristic function of electron energy losses is determined in this way:

$$-I_m \left(\frac{1}{\varepsilon} \right) = \frac{\varepsilon_i}{\varepsilon_i^2 + \varepsilon_r^2}.$$

The spectral characteristic of the imaginary part of the inverse value of complex dielectric penetrability $\left(I_m \left(-\varepsilon^{-1} \right) \right)$ is displayed in Fig.5a. It is seen from here that no clearly marked maxima and minima are observed at $e_{\parallel c}$ polarization, i.e $\left(I_m \left(-\varepsilon^{-1} \right) \right)$ rises over a wide range of energies from 0 to 6,3 eV and decreases over a narrow energy range.

At $e_{\perp c}$ polarization $\left(I_m \left(-\varepsilon^{-1} \right) \right)$ at first grows, an arm is detected in the 3,0 – 4,7 eV interval, a clearly marked

maximum is present at 6,01 eV a minimum at the energy of 6,75 eV.

The effective state density is expressed by the formula below

$$g_{eff} = \varepsilon_i (\hbar \omega)^2,$$

and the results of computing at $e_{\parallel c}$ and $e_{\perp c}$ polarizations are given in Fig.5b. As follows from Fig.5b, at $e_{\parallel c}$ polarization g_{eff} slightly increases in the 5.82-6.83 eV range, smeared maxima are witnessed at the energies of 3,82 and 5,36 eV and minimum at 5,82 eV. An arm is observed on the g_{eff} versus – energy dependence curve in the 3-3,4 eV range at $e_{\perp c}$ polarization, a maximum takes place at 4,67 eV and a minimum occurs at 5,95eV. An abrupt rise in the 6 -6,5eV range and a slight decrease in g_{eff} are noted.

IV. CONCLUSION

So, in this report the spectra of optical fundamental functions of the semiconductor SnS have been calculated for two polarizations $e_{\parallel c}$ and $e_{\perp c}$ in 0 - 8 eV energy range for the first time. Parameters have been defined, effective masses of electrons and holes of compound were calculated on the basis of the band structure. The results obtained allow a detailed analysis of the optical properties and electronic structure of SnS

REFERENCE

- [1] Konstantinov O. V., Nasibullaev Sh. K., Panakhov M. M. Ob analiticheskom virajenii dlya formfaktorov psevdopotensiala //Semiconductors, 1977, т. 11, №5, с. 881-885.
- [2] Austin B., Heine V., Sham L.J. General theory of pseudopotentials // Phys. Rev., 1962, v.127, №7, pp.276-282.
- [3] Bachelet G.B., Hamann D.R., and Schluter M. Pseudopotentials that work: From H to Pu // Phys. Rev., 1982, B26, №8, pp. 4199-4223.
- [4] Phylipps J.C. Energy-band interpolation scheme based on a pseudopotential // Phys. Rev., 1958, v. 112, №3, pp.685-695.
- [5] German F. Calculation of the energy band structures of the diamond and germanium crystals by the method of orthogonalized plane waves // Phys. Rev., 1954, v. 93, №6, pp.1214-1225.
- [6] Phylipps J.C., Kleinman L. New method for calculating wave function in crystals and molecules // Phys. Rev., 1959, v. 116, №2, pp. 287-294.
- [7] Qashimzadeh F.M., Khartsev V.E. Spekr valentnoy zoni anizotropnoqo SnS // Physics of the Solid State, 1962, 4, c.434-442.
- [8] Uxanov Yu.I. Optical properties of semiconductors. M. Nauka, 1977, 366p. (68)